Available online at www.sciencedirect.com
ScienceDirect
International Journal of Mass Spectrometry 269 (2008) 138–144
International Journal of Mass Spectrometry
www.elsevier.com/locate/ijms

ESI-MS and theoretical study on the coordination structures and reaction modes of the diperoxovanadate complexes containing histidine-like ligands

Xian-Yong Yu [a,c,d], Xin Xu [b,c,*], Zhong Chen [b,c,*,1]

[a] School of Chemistry and Chemical Engineering, Hunan University of Science and Technology, Xiangtan 411201, China
[b] Departments of Chemistry and Physics, Xiamen University, Xiamen 361005, China
[c] State Key Laboratory for Physical Chemistry of Solid Surface, Xiamen 361005, China
[d] Key Laboratory of QSAR/QSPR (Hunan University of Science and Technology, Xiangtan 411201), College of Hunan Province, China

Received 31 July 2007; accepted 29 September 2007
Available online 13 October 2007

Abstract

In order to study the coordination structures and the reaction modes of diperoxovanadate complexes in the gas phase, the interaction between $K_3[OV(O_2)_2(C_2O_4)]\cdot H_2O$ and a series of histidine-like ligands has been investigated by the combination of the electrospray ionization-mass spectrometry (ESI-MS) and the density functional theory (DFT) calculations. The experimental results proved the formation of both $[OV(O_2)_2L]^-$ (L = all histidine-like ligands) and $[OV(O_2)_2L'_2]^-$ (L′ = histidine and carnosine only) species. DFT calculations at the level of B3LYP/6-31+G* showed that $[OV(O_2)_2L'_2]^-$ is a hexa-coordinated complex, instead of a hepta-coordinated complex as proposed before. The unique coordination mode in the gas phase is for one ligand to bind to the oxygen atoms via hydrogen binding, rather than both ligands to the metal center. The L'_2 dimer formation and the maintenance of the hydrogen bonding within the dimer during the complex formation are two important factors that enhance the abundance of the $[OV(O_2)_2L'_2]^-$ species. The calculated bonding enthalpy and free energy changes provided an explanation on the reaction modes of the interaction systems, in agreement with the observations of the ESI-MS experiments.

Keywords: ESI-MS; DFT calculation; Peroxovanadate complex; Histidine-like ligand

1. Introduction

Peroxovanadate complexes are well-known effective oxidants of hydrocarbons, alcohols and thioethers, etc., usually leading to good product yield with high selectivity in mild conditions [1–5]. Recently, these compounds have drawn renewed attention, as they may be used as insulin-mimetic agents in the treatment of human diabetes [1–5,9,10], and have a potential as anti-tumor drugs [1–5]. There exist many studies [5–38], not only on the syntheses and characterization of the peroxovanadate compounds, but also on their biological mechanism. Coordination chemistry of the peroxovanadate complexes is also of main concern [14–32]. For example, Tracey and co-workers have used nuclear magnetic resonance (NMR) spectroscopy to explore the coordination reactions between peroxovanadate complexes and a series of amino acids or peptides [24,25]. They studied the reaction kinetics thoroughly and obtained much information about the peroxovanadate complexes such as formation constants and coordination mechanism in solutions. Pettersson and co-workers have used potentiometric and ^{51}V NMR methods to investigate the $H^+/H_2VO_4^-/H_2O_2$/ligand systems in detail and obtained the distribution of the peroxovanadate species in solutions [26–32]. In our previous work, we have performed a combined experimental and density functional theory (DFT) study on the interaction systems between diperoxovanadate and a series of organic ligands in solutions [15]. Our results concluded that the newly formed peroxovanadate species in solutions were $[OV(O_2)_2L'''']^{n-}$ (L′′′′ = organic ligands) with the ligands being coordinated to the metal, sug-

* Corresponding authors at: Departments of Chemistry and Physics, Xiamen University, Xiamen 361005, China. Tel.: +86 592 2182219; fax: +86 592 2183047.
E-mail addresses: xinxu@xmu.edu.cn (X. Xu), chenz@jingxian.xmu.edu.cn (Z. Chen).
[1] Tel.: +86 592 2181712; fax: +86 592 2189426.

1387-3806/$ – see front matter © 2007 Elsevier B.V. All rights reserved.
doi:10.1016/j.ijms.2007.09.022

gesting a 1:1 molar ratio between vanadium and the organic ligands [10,15,19–23].

Conte and co-workers have performed a combined study by using the electrospray ionization-mass spectrometry (ESI-MS), ^{51}V NMR, and ab initio calculations to investigate the NH_4VO_3/H_2O_2/histidine-like ligand systems [33,34]. Besides the 1:1 $[OV(O_2)_2L'''']^{n-}$ species which also existed in the solution phase, the $[OV(O_2)_2L_2''']^{n-}$ species were also detected in high relative abundance in the gas phase by the ESI-MS experiments. Ab initio calculations at the level of Hartree–Fock with the 3-21G* basis set showed that the ligands were both coordinated to the vanadium atom in $[OV(O_2)_2L_2''']^{n-}$, making a hepta-coordinated vanadium. Although a hepta-coordinated vanadium has been reported before [37,38], it is less common, as compared to hexa-coordination, in the vanadium chemistry, suggesting that the gas-phase coordination chemistry may be different from that in solutions.

In this work, we have studied the coordination structures and the reaction modes of the diperoxovanadate complexes in the gas phase. The interaction between $K_3[OV(O_2)_2(C_2O_4)]\cdot H_2O$ {abbr. bpV(oxa)} and a series of histidine-like ligands {imidazole, 2-methyl-imidazole, 4-methylimidazole, histidine, and carnosine (abbr. Imi, 2-Me-Imi, 4-Me-Imi, His, and Carn, respectively)} has been investigated in detail by the combination of ESI-MS and DFT calculations. In consistency with the results of Conte and co-workers [33,34], both peroxovanadate species $[OV(O_2)_2L]^-$ (L = all histidine-like ligands) and $[OV(O_2)_2L_2']^-$ (L′ = His and Carn only) were observed in the gas phase by the ESI-MS experiments. DFT calculations at the level of B3LYP/6-31+G* suggested that, unlike that in solutions where the ligand bind to the center metal, the favorable coordination mode in the gas phase is for the ligand to bind to the oxygen atoms of bpV via hydrogen binding. The abundance of the $[OV(O_2)_2L_2']^-$ species is related to the feasibility of L_2' dimer formation and the retainable hydrogen bonding within the dimer when coordinated to the peroxovanadate. The calculated bonding enthalpy and free energy changes provided an explanation on the reaction modes of the interaction systems, in agreement with the observations of the ESI-MS experiments.

2. Experimental and theoretical

2.1. Materials and preparation

The diperoxovanadate complex bpV(oxa), was prepared according to the literature [39]. The histidine-like ligands (Imi, 2-Me-Imi, 4-Me-Imi), as well as His and Carn are all commercial products.

2.2. ESI-MS spectroscopy

ESI-MS was measured by a Finnigan MAT LCQ instrument with the following parameters: sheath gas (N_2) 32 mL/min, aux gas (N_2) 5 mL/min, capillary temperature 170–180 °C, discharge voltage 2.52–2.55 kV, spray voltage 3.6 kV, capillary voltage −4.0 kV, and scan range 50–800 *m/z*. Flow rate of mobile phase was set to 0.2–0.8 mL/min. The solutions of the interaction systems between bpV(oxa) complex (1×10^{-2} mol/L) and ligands with 1:3 molar ratios in EtOH/H_2O (1:1 volume ratio) solution were introduced into the instrument by direct injection. The ESI-MS results are represented in Fig. 1 and Table 1.

2.3. Computational method

All quantum mechanics (QM) calculations were performed using the B3LYP hybrid density functional, which includes a mixture of Hartree–Fock exchange with Becke88 exchange functional under the generalized gradient approximation plus a mixture of Vosko–Wilk–Nusair local correlation functional and Lee–Yang–Parr nonlocal correlation functional [40–42]. B3LYP method generally provides good descriptions of reaction profiles, including geometries, heats of reactions, and barrier heights [43], although it may systematically underestimate the strength of hydrogen bondings [44].

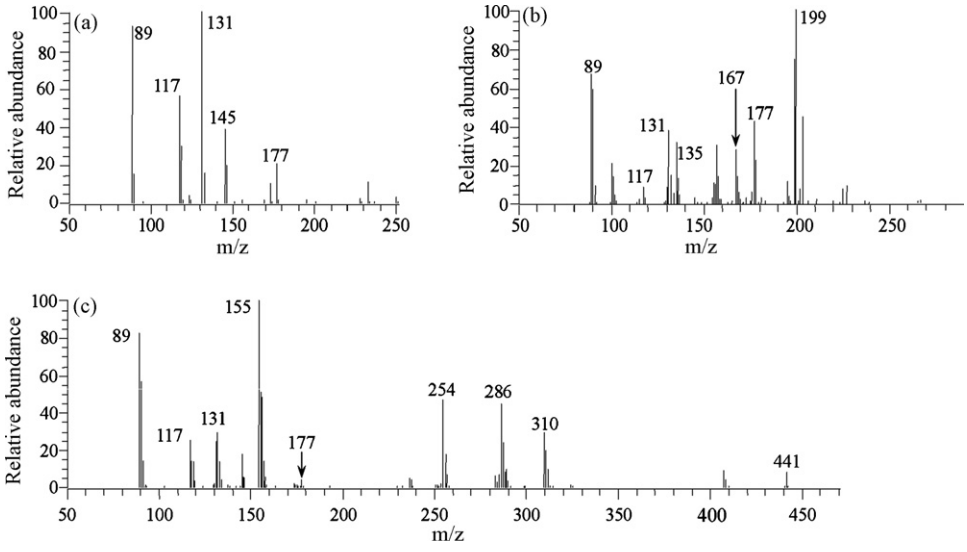

Fig. 1. ESI-MS spectra of bpV(oxa) (a) and the interaction system between bpV(oxa) and imidazole (b) or histidine (c) with 1:3 molar ratio.

Table 1
Relative abundances of $[OV(O_2)_2]^-$ and $[OV(O_2)_2L_n]^-$ ($n = 1, 2$) in the ESI-MS experiments of interaction systems with 1:3 molar ratio

Systems c(V) = 1×10^{-2} mol/L	Species	*m/z*	Relative abundances (%) bpV(oxa): L = 1:3
bpV(oxa) + Imi	$[OV(O_2)_2]^-$	131	38
	$[OV(O_2)_2(Imi)]^-$	199	100
bpV(oxa) + 2-Me-Imi	$[OV(O_2)_2]^-$	131	50
	$[OV(O_2)_2(2\text{-Me-Imi})]^-$	213	15
bpV(oxa) + 4-Me-Imi	$[OV(O_2)_2]^-$	131	81
	$[OV(O_2)_2(4\text{-Me-Imi})]^-$	213	44
bpV(oxa) + His	$[OV(O_2)_2]^-$	131	29
	$[OV(O_2)_2(His)]^-$	286	44
	$[OV(O_2)_2(His)_2]^-$	441	8
bpV(oxa) + Carns	$[OV(O_2)_2]^-$	131	7
	$[OV(O_2)_2(Carns)]^-$	357	100
	$[OV(O_2)_2(Crans)_2]^-$	583	22

We used the Wadt and Hay effective core potential [45] for the metal center (13 explicit electrons for the neutral vanadium atom) with the valence double zeta contraction of the basis functions (denoted as Lacvp+* in Jaguar [46]). For O, N, C and H, we used the standard 6-31+G* basis sets developed by Pople and co-workers [47].

All calculations were carried out with the Jaguar program [46]. We performed geometry optimization to locate the stationary points on the potential surface using the Berny algorithm. The optimized geometries are shown in Figs. 2 and 3. Analytical vibrational frequencies were calculated to ensure that each minimum in the gas phase is a true local minimum (only real frequencies). All energies reported in this work are ΔH (298 K) and ΔG (298 K) in kcal/mol as summarized in Table 2 and Figs. 4 and 5.

3. Results and discussion

3.1. ESI-MS study on the interaction systems

Data, reported in Table 1, were obtained for solutions of the interactions systems containing weighted amounts of peroxovanadate and histidine-like ligands in EtOH/H_2O (1:1). The electrospray mass spectra of these solutions, obtained by direct infusion into the ESI source, show the occurrence of different species [33,34]. Most of the observed peaks can be attributed to the vanadate species with different coordination sphere. For example, in the ESI-MS spectrum of the bpV(oxa) solution, peaks of $[HC_2O_4]^-$ (*m/z* 89, relative abundance 94%), $[O_3V(H_2O)]^-$ (*m/z* 117, 56%), $[OV(O_2)_2]^-$ (*m/z* 131, 100%), $[O_3V(EtOH)]^-$ (*m/z* 145, 39%), and $[OV(O_2)_2(EtOH)]^-$ (*m/z* 177, 21%) were observed (Fig. 1a). While in the spectrum of the solution of bpV(oxa) (1×10^{-2} mol/L) and imidazole in a 1:3 molar ratio, new peaks of $[2Imi\text{-}H]^-$ (*m/z* 135, 32%), $[O_3V(Imi)]^-$ (*m/z* 167, 27%) and $[OV(O_2)_2(Imi)]^-$ (*m/z* 199, 100%) appeared (see Fig. 1b). When the ligand used was histidine, new peaks of $[His]^-$ (*m/z* 155, 100%), $[O_3V(His)]^-$ (*m/z* 254, 47%), $[(His)_2]^-$ (*m/z* 310, 29%), $[OV(O_2)_2(His)]^-$ (*m/z* 286, 44%), and $[OV(O_2)_2(His)_2]^-$ (*m/z* 441, 8%) were observed, indicating the formation of the new species, as shown in Fig. 1c.

The ESI-MS experiments demonstrate the formation of the $[OV(O_2)_2L]^-$ species [48]. This indicates that there is a direct coordination pathway between $[OV(O_2)_2]^-$ and L in the gas phase; this also indicates that there exists a competitive coordination to the V center between the solvent molecules EtOH/H_2O and the L ligands. For example, the relative abundances of

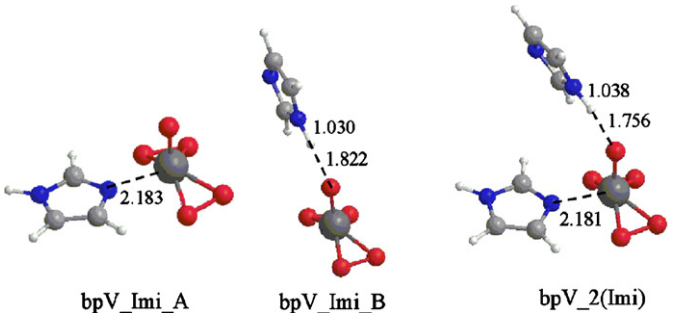

Fig. 2. Optimized structures for the $[OV(O_2)_2(Imi)]^-$ and $[OV(O_2)_2(Imi)_2]^-$ species. Here bpV = $[OV(O_2)_2]^-$ and Imi = imidazole.

Table 2
Coordination reactions for the formation of the $[OV(O_2)_2L_n]^-$ ($n = 1, 2$) and species. ΔH_{298} and ΔG_{298} are in kcal/mol

Coordination reactions[a]		ΔH_{298}	ΔG_{298}
bpV + Imi → bpV_Imi_A	(1)	−9.42	2.09
bpV + Imi → bpV_Imi_B	(2)	−15.64	−7.79
bpV_Imi_A + Imi → bpV_2(Imi)	(3)	−19.89	−8.40
bpV_Imi_B + Imi → bpV_2(Imi)	(4)	−13.67	1.48
bpV + 2Imi → bpV_2(Imi)	(5)	−29.31	−6.31
Imi + Imi → $(Imi)_2$	(6)	−7.26	−0.47
bpV + His → bpV_His_A	(7)	−8.89	2.64
bpV + His → bpV_His_B	(8)	−24.42	−13.66
bpV_His_A + His → bpV_2(His)	(9)	−27.75	−13.25
bpV_His_B + His → bpV_2(His)	(10)	−12.22	3.05
His + His → $(His)_2$	(11)	−14.30	−3.37
bpV + $(His)_2$ → bpV_$(His)_2$_A	(12)	−20.27	−4.15
bpV + $(His)_2$ → bpV_$(His)_2$_B	(13)	−10.23	4.16
bpV_His_A + His → bpV_$(His)_2$_A	(14)	−25.68	−10.16
bpV_His_A + His → bpV_$(His)_2$_B	(15)	−15.64	−1.85
bpV + 2His → bpV_2(His)	(16)	−36.64	−10.61

[a] Here bpV = $[OV(O_2)_2]^-$ and L = imidaozle and histidine. See Figs. 2 and 3 for structures.

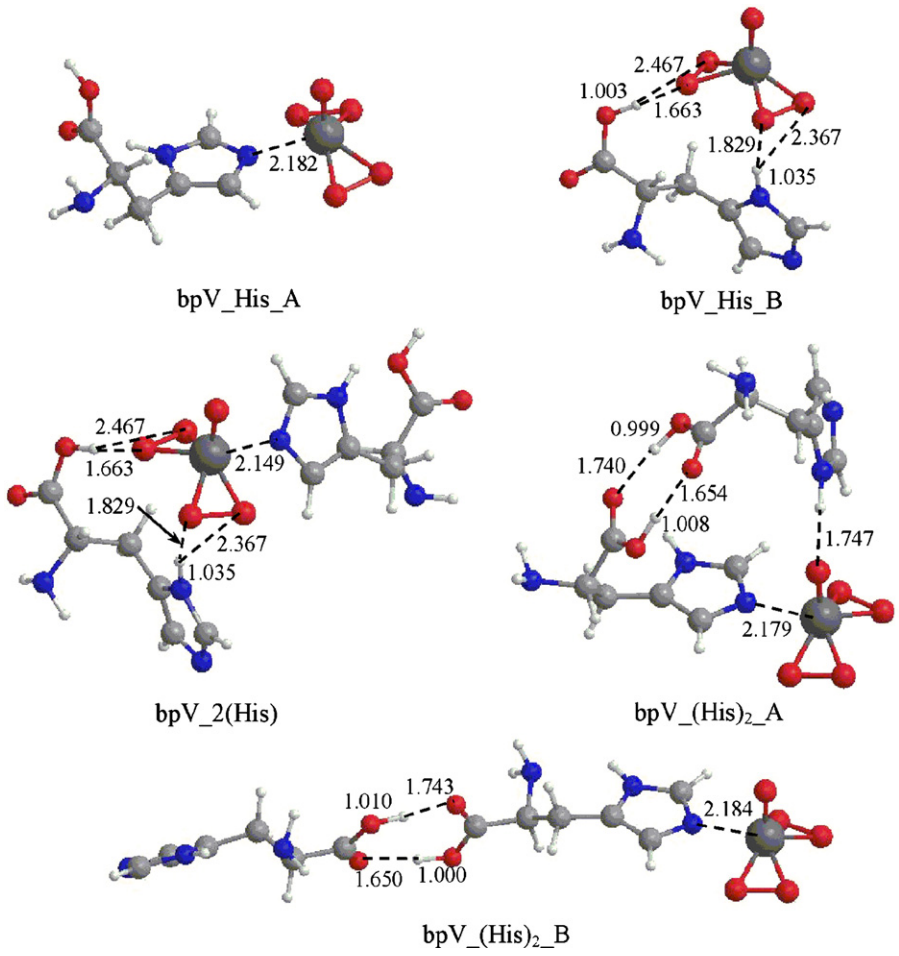

Fig. 3. Optimized structures for the $[OV(O_2)_2(His)]^-$ and $[OV(O_2)_2(His)_2]^-$ species. Here bpV = $[OV(O_2)_2]^-$ and His = histidine.

$[OV(O_2)_2]^-$ and $[OV(O_2)_2(EtOH)]^-$ were reduced from 100 and 21% to 29 and 4%, respectively, due to the formation of the $[OV(O_2)_2(His)]^-$ species. The formation of the 1:1 ratio of the $[OV(O_2)_2L]^-$ species is in line with the observation in the NMR experiments of our pervious studies [15].

When the ligands were His and Carn rather than the histidine-like ligands such as Imi, 2-Me-Imi, 4-Me-Imi, the $[OV(O_2)_2L'_2]^-$ species were also observable with relatively high abundance (see Table 1). This is at odds with the results in solutions, which showed that only the 1:1 molar ratio complexes of $[OV(O_2)_2L''']^-$ were observable. Similar ESI-MS results were obtained by Conte and co-workers for the NH_4VO_3/H_2O_2/histidine-like ligand systems [33,34]. Their ab initio calculations at the level of Hartree–Fock/3-21G* suggested a hepta-coordinated vanadium complex, whose structure is, however, less common [37,38], as compared to hexa-coordination in the vanadium coordination chemistry.

3.2. Theoretical study on the interaction systems

We took imidazole and histidine as the representative ligands for these two types of interaction systems. We optimized the $[OV(O_2)_2(Imi)]^-$ species, and obtained two local minima of different geometric structures. One geometry, labeled as bpV_Imi_A, is with the N coordination to the V metal atom, whose imidazole ring is in the equatorial direction with respect to the oxygen atoms of the peroxide groups (shown in Fig. 2). The binding enthalpy is calculated to be 9.42 kcal/mol (see Fig. 4). In terms of free energy change, however, this complexation process is uphill by 2.09 kcal/mol (see Fig. 5), indicating that the binding energy gain may not be compensable for the entropy loss. The structure of bpV_Imi_A has been pointed out before by Conte and co-workers [34]. The other geometry, labeled as bpV_Imi_B, is a hydrogen bonding complex, in which the N–H group in the imidazole is coordinated to the oxo group of the metal center (see Fig. 2). The binding enthalpy is calculated to be 15.64 kcal/mol (see Fig. 4). Thus, bpV_Imi_B is 6.22 kcal/mol more stable than bpV_Imi_A. The free energy change for this process is downhill by 7.79 kcal/mol (see Fig. 5), suggesting that the formation of the hydrogen bonded complex, bpV_Imi_B, is a favorable process.

Worthy of note is the optimization of the $[OV(O_2)_2(Imi)_2]^-$ species. We were unable to locate the hepta-coordination complex as pointed out by Conte and co-workers [34]. We did find such a complex at the level of Hartree–Fock with 3-21G*. Thus, we suspected that the hepta-coordination complex is an artifact due to the omission of the correlation effects and the limitation of the 3-21G* basis set. At the level of B3LYP/6-31+G*, we found that one imidazole ring is coordinated to the vanadium atom, as

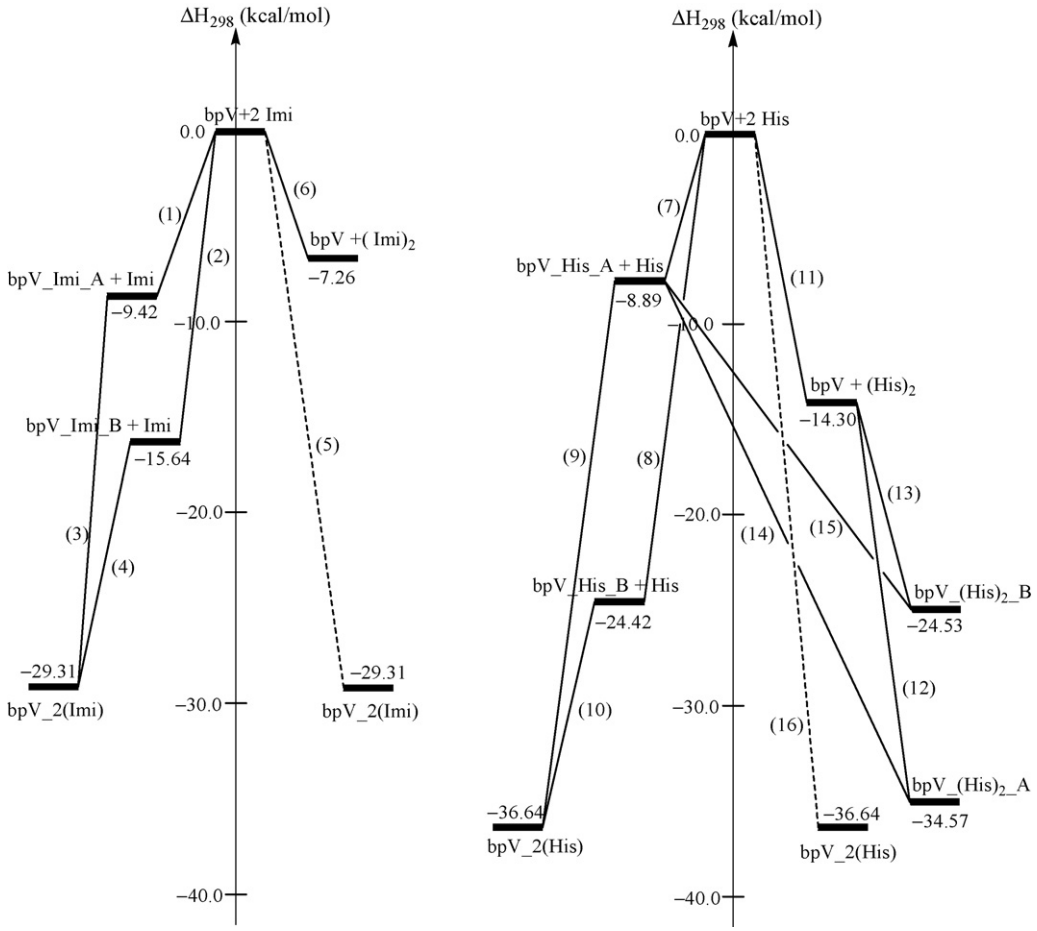

Fig. 4. Enthalpy changes for the formation of the $[OV(O_2)_2L]^-$ and $[OV(O_2)_2L_2]^-$ species. Here bpV = $[OV(O_2)_2]^-$ and L = imidazole (abbr. Imi) and histidine (abbr. His). The dotted lines refer to the three body processes of Eqs. (5) and (16) as summarized in Table 2.

is seen in bpV_Imi_A; the other imidazole ring is bound to the oxygen of the metal oxo group via hydrogen bonding, similar to that in bpV_Imi_B. The net binding enthalpy with respect to bpV and two free imidazole ligands is 29.31 kcal/mol (Fig. 4). And we denoted this $[OV(O_2)_2(Imi)_2]^-$ species as bpV_2(Imi) (see Fig. 2).

Our calculations showed that two imidazole ligands can dimerize with the N–H group of one imidazole pointing to the N atom of the other imidazole. The net binding enthalpy is 7.26 kcal/mol with $\Delta G_{298} = -0.47$ kcal/mol. This is in accord with the experimental observation of the $[2Imi\text{-}H]^-$ (m/z 135) peak with relative abundance of 32% (see Fig. 1b). However, we were unable to locate a complex with an imidazole dimer directly coordinating to bpV to form bpV_$(Imi)_2$. Coordination of the imidazole dimer to the metal tended to break the hydrogen bond between two imidazole ligands. We might estimate the binding enthalpy for an imidazole dimer with a frozen geometry to be ∼8 kcal/mol, which is, however, ∼15 kcal/mol less stable than bpV_2(Imi). We also anticipate that such a way of complexation is entropy unfavorable as it is for the formation of bpV_Imi_A.

Similarly, we found two binding geometries for the $[OV(O_2)_2(His)]^-$ species (Fig. 3). One is labeled as bpV_His_A, where the histidine ligand coordinates to the vanadium atom in the same way as the imidazole ligand in bpV_Imi_A. Its binding enthalpy is calculated to be 8.89 kcal/mol (Fig. 4). Again entropy loss is larger than the enthalpy gain, making such a complexation process unfavorable (Fig. 5). The other one, labeled as bpV_His_B, is also a hydrogen bonded complex. However, it differs from bpV_Imi_B in that the histidine ligand binds to two peroxide oxygens by using its N–H group in the imidazole ring and its O–H group in the carboxylic group, respectively (see Fig. 3) to form a multi hydrogen bond complex. The net binding enthalpy is as great as 24.42 kcal/mol, being 15.53 larger than that in bpV_His_A. The free energy change (−13.66 kcal/mol) demonstrates that this is a feasible process.

Again, we were unable to locate a hepta-coordinated complex. Instead we found the vanadium metal center remains in the hexa-coordination. The geometry of the $[OV(O_2)_2(His)_2]^-$ species, labeled as bpV_2(His), may be viewed as a combination of bpV_His_A and B (Fig. 3). The binding enthalpy for bpV_2(His) with respect to bpV and two free histidine ligands is 36.64 kcal/mol (Fig. 4).

In the ESI-MS spectrum of the bpV and histidine interaction system, we observed the $[(His)_2]^-$ species with a relative abundance of 29%. Indeed we calculated the dimerization enthalpy of two histidine ligands via their carboxyl groups as 14.30 kcal/mol with $\Delta G_{298} = -3.37$ kcal/mol. And we found two binding struc-

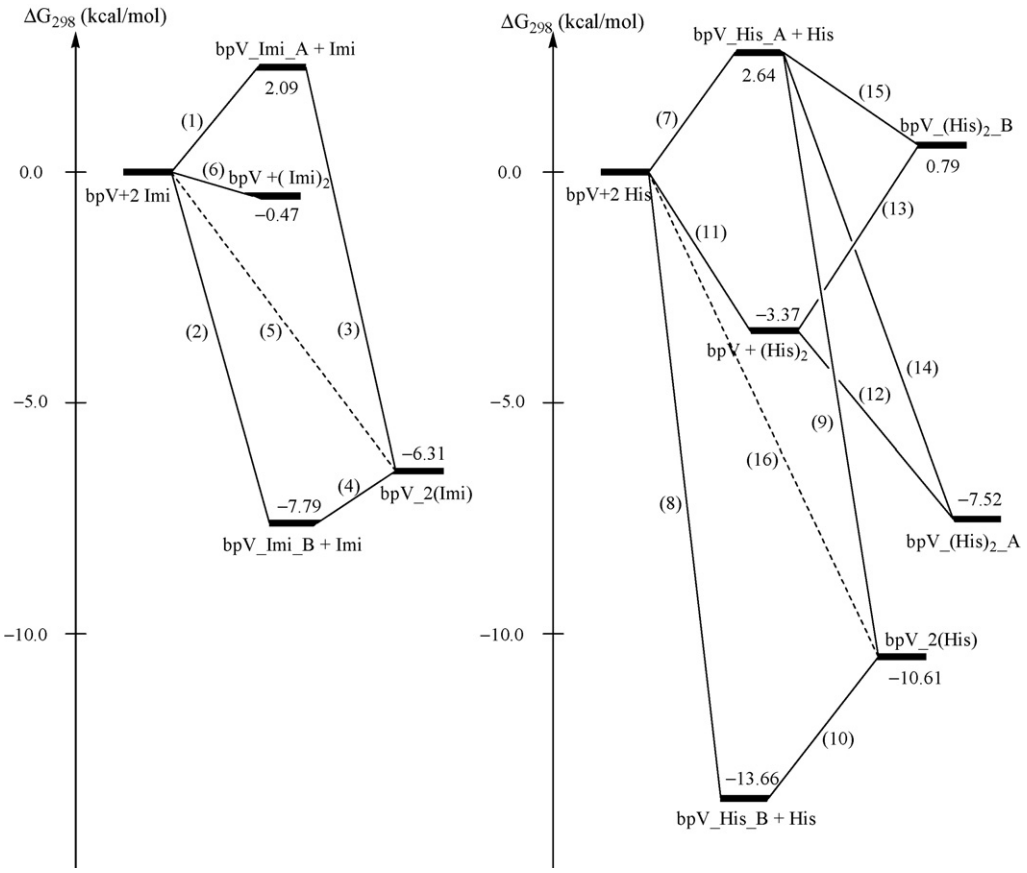

Fig. 5. Free energy changes for the formation of the $[OV(O_2)_2L]^-$ and $[OV(O_2)_2L_2]^-$ species. Here bpV = $[OV(O_2)_2]^-$ and L = imidazole (abbr. Imi) and histidine (abbr. His). The dotted lines refer to the three body processes of Eqs. (5) and (16) as summarized in Table 2.

tures, labeled as bpV_$(His)_2$_A and B (see Fig. 3), which could be viewed as a complex between a histidine dimer and bpV, with binding enthalpy of 20.27 and 10.23 kcal/mol, respectively. The geometry of bpV_$(His)_2$_A species is similar to that of bpV_2(Imi) in that one N–H group of the imidazole ring binds to the oxygen of the metal oxo group and the N atom in the other imidazole ring binds to the vanadium metal center. Thus, the histidine ligands distinguish from the imidazole ligands in that histidine dimer can binds to bpV to form a stable complex with retainable hydrogen bonds within the dimer. We emphasize here that bpV_$(His)_2$_A formation is all the way downhill in terms of ΔG_{298}.

3.3. Reaction modes on the interaction systems

Table 2 summarizes the coordination reactions, possibly occurring when bpV interacts with ligands. During the reactions, the $[OV(O_2)_2L]^-$ species may be formed, which may subsequently reacts with another ligand to form the $[OV(O_2)_2L_2]^-$ species. The abundance of the final products may be related to the stabilities of the corresponding complexes. As the bonding enthalpy in bpV_2(His) is 7.33 kcal/mol stronger than that in bpV_2(Imi), we expect that the abundance of the former species is higher than that of the latter. From Table 2 and Figs. 4 and 5, we see that there are three routes to bpV_2(Imi) or bpV_2(His). However, except (5) or (16), both (1) → (3) and (2) → (4) or (7) → (9) and (8) → (10) contain reactions with positive ΔG_{298}.

The direct three body reaction between a bpV and two free ligands shall be rare due to the limited collision probability. However, if the two free ligands can dimerize first, a new channel for bpV to react with L_2 is operative, which shall greatly enhance the formation probability of $[OV(O_2)_2L_2]^-$. Both imidazole and histidine have ability to dimerize. The bonding enthalpy is 7.26 and 14.30 kcal/mol for $(Imi)_2$ and $(His)_2$, respectively. Most importantly, when the histidine dimer binds to bpV, the dimer bond is retained, leading to the formation of bpV_$(His)_2$_A with negative ΔG_{298}. On the other hand, when the imidazole dimer binds to bpV, the dimer bond will be broken, leading to no formation of complex between bpV and $(Imi)_2$. Thus, we anticipate that the abundance of $[OV(O_2)_2L_2]^-$ is high for the systems using the histidine ligands. Indeed in their ESI-MS experiments, Conte and co-workers reported a relative abundance of $[OV(O_2)_2(Imi)_2]^- < 1\%$ [33] or 4% [34] and that of $[OV(O_2)_2(His)_2]^-$ of 25% [33,34]; whereas our ESI-MS experiments hardly detected any occurrence of $[OV(O_2)_2(Imi)_2]^-$, $[OV(O_2)_2$(2-Me-Imi)$_2]^-$, and $[OV(O_2)_2$(4-Me-Imi)$_2]^-$, but abundances of $[OV(O_2)_2(His)_2]^-$ of 8% and $[OV(O_2)_2(Carns)_2]^-$ of 22%, in agreement with the theoretical deduction.

4. Conclusions

ESI-MS together with DFT calculations have been employed to study the interaction systems between bpV(oxa) and the histidine-like ligands. Although ESI-MS is powerful in detecting the existence of a specific species with its abundance to indicate the relative stability, ESI-MS provides no information on the binding structure of the given species. Our DFT calculations complement the ESI-MS experiments, showing that there are competitive interactions among different ligands to coordinate to bpV and the coordination modes are different in solutions and in the gas phase. For the $[OV(O_2)_2L]^-$ species in solutions, the favorite coordination mode is for the ligand to bind to the metal center to form a N–V bond [10,15,19–23,27,28,30,31]; whereas, based on the free energy change, we find that the favorable process in the gas phase is for the ligand to bind to the oxygen atoms of bpV via hydrogen binding. We confirm that the $[OV(O_2)_2L'_2]^-$ species in the gas phase is also observable, in agreement with the finding of Conte and co-workers [33,34]. Our calculations reveal that only one ligand is directly coordinated to the vanadium atom, while the other one prefers to bind to the metal oxo group via hydrogen bonding. The relative abundance of the $[OV(O_2)_2L'_2]^-$ species in ESI-MS is decided by both the binding energy and the collision probability between the peroxovanadate species and the histidine-like ligands. Especially, a new channel is operative, if the two free ligands can dimerize first, and the dimer can coordinate to bpV without breaking the hydrogen bonds within the dimmer. We believe that our present results, combined with our previous results in solutions [10,15,19–23], should be useful for the understanding of the coordination chemistry of vanadium, which enriches the existing literatures [5–38].

Acknowledgements

This work was supported by National Natural Science Foundation of China (20525311, 10774126, 20423002, and 20772027); the Ministry of Science and Technology of China (2004CB719902, 2007CB815206); Key Project of Health and Science and Technology of Xiamen (Wkj2005-2-019); Science Research Foundation of Ministry of Health & United Fujian Provincial Health and Education Project for Tackling the Key Research (3502Z20051027); Project supported by Hunan Provincial Natural Science Foundation of China (06JJ30004); China Postdoctoral Science Foundation (20070410805).

References

[1] K.H. Thompson, C. Orvig, Science 300 (2003) 936.
[2] K.H. Thompson, J.H. McNeill, C. Orvig, Chem. Rev. 99 (1999) 2561.
[3] A. Butler, J.V. Walker, Chem. Rev. 93 (1993) 1937.
[4] D.C. Crans, J.J. Smee, E. Gaidamauskas, L.Q. Yang, Chem. Rev. 104 (2004) 849.
[5] B.I. Posner, R. Faure, J.W. Burgess, A.P. Bevan, D. Lachance, G.Y. Zhang-Sund, I.G. Fantus, J.B. Ng, D.A. Hall, B.S. Lum, A. Shaver, J. Biol. Chem. 269 (1994) 4596.
[6] G. Zampella, P. Fantucci, V.L. Pecoraro, L. De Gioia, Inorg. Chem. 45 (2006) 7133.
[7] G.J. Colpas, B.J. Hamstra, J.W. Kampf, V.L. Pecoraro, J. Am. Chem. Soc. 116 (1994) 3627.
[8] G.J. Colpas, B.J. Hamstra, J.W. Kampf, V.L. Pecoraro, J. Am. Chem. Soc. 118 (1996) 3469.
[9] D.C. Crans, A.D. Keramidas, H. Hoover-Litty, O.P. Anderson, M.M. Miller, L.M. Lemoine, S. Pleasic-Williams, M. Vandenberg, A.J. Rossomando, L.J. Sweet, J. Am. Chem. Soc. 119 (1997) 5447.
[10] X.Y. Yu, S.H. Cai, Z. Chen, J. Inorg. Biochem. 99 (2005) 1945.
[11] C. Hiort, J. Goodisman, J.C. Dabrowiak, Biochemistry 35 (1996) 12354.
[12] D.W.J. Kwong, O.Y. Chan, R.N.S. Wong, S.M. Musser, L. Vaca, S.I. Chan, Inorg. Chem. 36 (1997) 1276.
[13] M. Sam, J.H. Hwang, G. Chanfreau, M.M. Abu-Omar, Inorg. Chem. 43 (2004) 8447.
[14] R.I. De La Rosa, M.J. Clague, A. Butler, J. Am. Chem. Soc. 114 (1992) 760.
[15] X.Y. Yu, S.H. Cai, X. Xu, Z. Chen, Inorg. Chem. 44 (2005) 6755.
[16] V. Conte, F. Di Furia, S. Moro, Tetrahedron Lett. 35 (1994) 7429.
[17] M. Andersson, V. Conte, F. Di Furia, S. Moro, Tetrahedron Lett. 36 (1995) 2675.
[18] V. Conte, F. Di Furia, S. Moro, S. Rabbolini, J. Mol. Catal. 113 (1996) 175.
[19] S.H. Cai, X.Y. Yu, Z. Chen, H.L. Wan, Chin. J. Chem. 21 (2003) 746.
[20] X.Y. Yu, S.H. Cai, Z. Chen, Spectrochim. Acta A 60 (2004) 391.
[21] X.Y. Yu, S.H. Cai, Z. Chen, Chin. J. Struct. Chem. 22 (2004) 511.
[22] T. Huang, S.H. Cai, X.Y. Yu, Z. Chen, Spectrochim. Acta A 64 (2006) 255.
[23] S.H. Cai, X.Y. Yu, Z. Chen, Spectrochim. Acta A 65 (2006) 616.
[24] A.S. Tracey, J.S. Jaswal, Inorg. Chem. 32 (1993) 4235.
[25] J.S. Jaswal, A.S. Tracey, J. Am. Chem. Soc. 115 (1993) 5600.
[26] H. Schmidt, I. Andersson, D. Rehder, L. Pettersson, J. Inorg. Biochem. 80 (2000) 149.
[27] H. Schmidt, I. Andersson, D. Rehder, L. Pettersson, Chem. - Eur. J. 7 (2001) 251.
[28] A. Gorzsas, I. Andersson, H. Schmidt, D. Rehder, L. Pettersson, Dalton Trans. (2003) 1161.
[29] A. Gorzsas, I. Andersson, L. Pettersson, Dalton Trans. (2003) 2503.
[30] L. Pettersson, I. Andersson, A. Gorzsas, Coord. Chem. Rev. 237 (2003) 77.
[31] I. Andersson, A. Gorzsas, L. Pettersson, Dalton Trans. (2004) 421.
[32] A. Gorzsas, K. Getty, I. Andersson, L. Pettersson, Dalton Trans. (2004) 2873.
[33] O. Bortolini, M. Carraro, V. Conte, S. Moro, Eur. J. Inorg. Chem. (1999) 1489.
[34] V. Conte, O. Bortolini, M. Carraro, S. Moro, J. Inorg. Biochem. 80 (2000) 41.
[35] O. Bortolini, V. Conte, F. Di Furia, S. Moro, Eur. J. Inorg. Chem. (1998) 1193.
[36] O. Bortolini, M. Carraro, V. Conte, S. Moro, Eur. J. Inorg. Chem. (2003) 42.
[37] V. Conte, F. Di Furia, G. Modena, in: W. Ando (Ed.), Organic Peroxides, J. Wiley & Son LTD., Chichester, UK, 1992, p. 559 (Chapter 11.2).
[38] V. Conte, O. Bortolini, in: Z. Rappoport (Ed.), The Chemistry of Peroxides, vol. 2, John Wiley & Sons, 2006, p. 1053.
[39] D. Begin, F.W.B. Einstein, J. Field, Inorg. Chem. 14 (1975) 1785.
[40] A.D. Becke, J. Chem. Phys. 98 (1993) 5648.
[41] C. Lee, W. Yang, R.G. Par, Phys. Rev. B 37 (1988) 785.
[42] S.H. Vosco, L. Wilk, M. Nusiair, Can. J. Phys. 58 (1980) 1200.
[43] J. Baker, M. Muir, J. Andzelm, A. Scheiner, in: B.B. Laird, R.B. Ross, T. Ziegler (Eds.), Chemical Applications of Density-Functional Theory, ACS Symp. Ser., vol. 629, American Chemical Society, Washington, DC, 1996.
[44] X. Xu, Q. Zhang, R.P. Muller, W.A. Goddard III, J. Chem. Phys. 122 (2005) 014105.
[45] P.J. Hay, W.R.J. Wadt, Chem. Phys. 82 (1985) 299.
[46] Jaguar 5.0, Schrödinger, Inc., Portland, Oregon, 2003.
[47] P.C. Hariharan, J.A. Pople, Chem. Phys. Lett. 16 (1972) 217.
[48] The ESI-MS experiments also demonstrate the formation of the $[O_3VL]^-$ species, which are not the focus of the present study and will be discussed elsewhere.